Reducing Domain Gap via Style-Agnostic Networks

Hyeonseob Nam*, HyunJae Lee*, Jongchan Park, Wonjun Yoon, Donggeun Yoo

Lunit Inc., Seoul, Korea
{hsnam,hjlee,jcpark,wonjun,dgyoo}@lunit.io

Abstract. Convolutional Neural Networks (CNNs) often fail to maintain their performance when they confront new test domains. This has posed substantial obstacles to real-world applications of deep learning. Recent studies suggest that one of the main causes of this problem is CNNs' inductive bias towards image styles (i.e. textures), which are highly dependent on domains, rather than contents (i.e. shapes). Motivated by this, we propose Style-Agnostic Networks (SagNets) which mitigate the style bias to generalize better under domain shift. Our experiments demonstrate that SagNets successfully reduce the style bias as well as domain discrepancy, and clarify a strong correlation between the bias and domain gap. Finally, SagNets achieve remarkable performance improvements in a wide range of cross-domain tasks, including domain generalization, unsupervised domain adaptation, and semi-supervised domain adaptation.

Keywords: Style Bias, Domain Generalization, Domain Adaptation

1 Introduction

Despite the huge success of Convolutional Neural Networks (CNNs) fueled by large-scale training data, their performance often degrades significantly when they encounter test data from unseen environments. This phenomenon, known as the problem of *domain shift* [42], comes from the distribution gap between training and testing domains. For a more reliable deployment of CNNs to ever-changing real-world scenarios, the community has long sought to make CNNs robust to domain shift under various problem settings such as Domain Generalization (DG) [30,9,5,8], Unsupervised Domain Adaptation (UDA) [34,11,47,35,43], and Semi-Supervised Domain Adaptation (SSDA) [7,50,45].

In stark contrast to the vulnerability of CNNs against domain shift, the human visual recognition system generalizes incredibly well across domains. For example, young children learn many object concepts from pictures, but they naturally transfer their knowledge to the real world [10]. Similarly, people can easily recognize objects in cartoons or paintings even if they have not seen the same style of an image before. Where does such a difference come from?

A recent line of studies has revealed that standard CNNs have an inductive bias far different from human vision: while humans tend to recognize objects

* Equal contribution

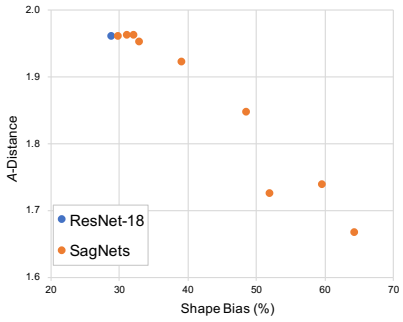

Fig. 1: Shape bias vs. domain gap. We train SagNets on 16-class-ImageNet [15] as a source domain and test on texture-shape cue conflict stimuli [14] as a target domain. Then we measure shape bias on the cue conflict stimuli and the $\mathcal{A}$-distance [4] between the two domains. SagNets not only successfully increase the shape bias and reduce domain discrepancy, but also reveal a strong correlation between the bias and domain gap. More details are in Sec. 4.1.

based on their contents (i.e. shapes) [28], CNNs exhibit a strong bias towards styles (i.e. textures) [1,14,21]. This may explain why CNNs are intrinsically more sensitive to domain shift because image styles are more likely to change across domains than image contents. Geirhos et al. [14] supported this hypothesis by showing that CNNs trained with heavy augmentation on styles become more robust against various image distortions. Researches on CNN architectures [41,29] have also demonstrated that adjusting the style information in CNNs helps to address multi-domain tasks.

In this paper, we propose *Style-Agnostic Networks (SagNets)* to enhance CNNs' transferability to different domains by reducing their bias towards styles (Fig. 2). Specifically, we construct separate content-biased and style-biased networks on top of a feature extractor. The content-biased network is encouraged to focus on contents rather than styles by randomizing styles in a latent feature space. The style-biased network is trained to focus on styles in the opposite way, and utilized to deactivate the styles of the feature extractor by adversarial learning. At inference time, the prediction is made by the combination of the feature extractor and the content-biased network, which consequently make decisions based on contents rather than styles.

Experiments with SagNets demonstrate that there exists an apparent correlation between CNNs' bias and their ability to handle domain shift: increasing shape bias reduces domain discrepancy (Fig. 1). Based on this property, SagNets make significant improvements in a wide range of scenarios including DG, UDA, and SSDA, achieving the state-of-the-art results on several cross-domain benchmarks. Furthermore, since our approach is orthogonal to other domain adaptation methods that explicitly align the source and the target distributions [11,35,45], it brings additional performance boosts when combined with those methods.

To summarize, our major contributions are as follows.

1. We propose Style-Agnostic Networks (SagNets), which effectively alleviate style bias of CNNs via two novel techniques: content-biased learning and adversarial style-biased learning.
2. We quantitatively examine the correlation between CNNs' bias and domain discrepancy, using 16-class-ImageNet [15] and texture-shape cue conflict

stimuli [14]. This confirms that concentrating on contents rather than styles reduces domain gap.
3. The effectiveness of SagNets is verified in various cross-domain tasks such as DG, UDA, and SSDA, on multiple datasets including PACS [30], Office-Home [48], and DomainNet [43], yielding substantial performance improvements.

2 Related Work

Bias Properties of CNNs. Our work is motivated by the recent findings that CNNs tend to learn styles rather than contents. Geirhos et al. [14] observed that standard ImageNet-trained CNNs are likely to make a style-biased decision on ambiguous stimuli (e.g. images stylized to different categories). Some studies [12,25] have also shown that CNNs perform well when only local textures are given while global shape structures are missing, but work poorly in the reverse scenario [3,14]. Many studies [23,14,21] have attempted to mitigate the style bias of CNNs under the assumption that it deteriorates CNNs' generalization capability. However, the practical impact of CNNs' bias on domain shift problems remains unclear, which we aim to explore in this paper.

Style Manipulation. We utilize convolutional feature statistics, namely the mean and variance, to control the style bias of CNNs. This owes to previous works dealing with the feature statistics in CNNs, mostly in generative frameworks to manipulate image styles. Gatys et al. [12] showed that feature statistics of a CNN effectively capture the style information of an image, which paved the way for neural style transfer [13,26,24]. In particular, adaptive instance normalization (AdaIN) [24] demonstrated that the style of an image can be easily changed by adjusting the mean and variance of convolutional feature maps. StyleGAN [27] recently produced impressive image generation results by repeatedly applying AdaIN operations in a generative network. Manipulating styles has also benefited discriminative problems. BIN [41] improved classification performance by reducing unnecessary style information using trainable normalization, and SRM [29] extended this idea to style-based feature recalibration.

Domain Generalization and Adaptation. Domain Generalization (DG) aims to make CNNs robust against novel domains outside the training distribution. A popular approach is learning a shared feature space across multiple source domains, for example, by minimizing Maximum Mean Discrepancy (MMD) [39,16] or adversarial feature alignment [32,33]. Some studies divide the model into domain-specific and domain-invariant components using low-rank parameterization [30] or domain-specific aggregation modules [9], assuming that the domain-invariant part can generalize to other domains. Meta-learning frameworks have also been explored in [2,8], where the source domains are split into meta-train and meta-test domains to simulate domain shift. Recently, JiGen [5] employed self-supervised signals such as solving jigsaw puzzles to improve generalization by learning invariant image regularities.

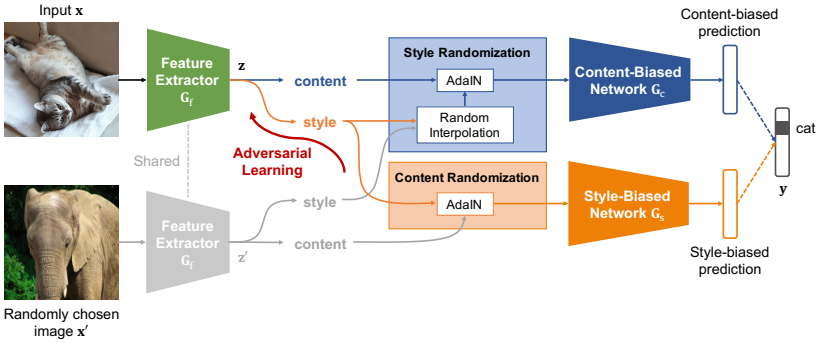

Fig. 2: Illustration of Style-Agnostic Networks (SagNets), where AdaIN refers to adaptive instance normalization [24]. SagNets reduce the style bias of a CNN by content-biased learning and adversarial style-biased learning, which makes the network more robust against domain shift.

Unsupervised Domain Adaptation (UDA) tackles the problem of domain shift where unlabeled data from the target domain are available for training. The mainstream approach is aligning the source and the target distributions by minimizing MMD [17,36], adversarial learning [11,47,35], or image-level translation [22,40]. Another problem setting with domain shift is Semi-Supervised Domain Adaptation (SSDA) where a few target labels are additionally provided. It is commonly addressed by simultaneously minimizing the distance between the domains as well as imposing a regularization constraint on the target data to prevent overfitting [7,50]. Recently, MME [45] optimized a minimax loss on the conditional entropy of unlabeled data and achieved the state-of-the-art performance.

Our approach is orthogonal to the majority of previous methods in that it does not explicitly deal with the discrepancy between the source domains nor between the source and the target domains (it does not even require any domain labels). Rather, we show that controlling the intrinsic bias of CNNs enhances their ability to generalize and adapt to different domains, which can complement a wide range of existing methods.

3 Style-Agnostic Networks

We present a general framework to make the network agnostic to styles but focused more on contents by end-to-end training (Fig. 2). It contains three networks: a feature extractor, a content-biased network, and a style-biased network. The content-biased network is encouraged to exploit image contents when making decisions by randomizing intermediate styles, which we call *Content-Biased Learning*. Conversely, the style-biased network is trained to be biased towards styles by randomizing contents, but it adversarially makes the feature extractor be less style-biased, which is referred to as *Adversarial Style-Biased Learning*. The prediction at test time is made by the feature extractor followed by the

content-biased network. Inspired by style transfer literature [13,26,24], we utilize summary statistics of CNN features as style representation and their spatial configuration as content representation.

3.1 Content-Biased Learning

In content-biased learning, we enforce the model to learn content-biased features by introducing a style randomization module. It randomizes the styles during training by interpolating the feature statistics between different examples regardless of their class labels. Consequently, the network is encouraged to be invariant to styles and biased toward contents in predicting the class labels.

Given an input training image $\mathbf{x}$ and a randomly selected image $\mathbf{x}'$, we first extract their intermediate feature maps $\mathbf{z}, \mathbf{z}' \in \mathbb{R}^{C\times H\times W}$ from the feature extractor $\mathbf{G}_\mathrm{f}$, where H and W indicate spatial dimensions, and C is the number of channels. Following [24,27,29], we compute the channel-wise mean and standard deviation $\mu(\mathbf{z}), \sigma(\mathbf{z}) \in \mathbb{R}^C$ as their style features:

$$\mu_c(\mathbf{z}) = \frac{1}{HW}\sum_{h=1}^{H}\sum_{w=1}^{W} z_{chw}, \tag{1}$$

$$\sigma_c(\mathbf{z}) = \sqrt{\frac{1}{HW}\sum_{h=1}^{H}\sum_{w=1}^{W}(z_{chw}-\mu_c(\mathbf{z}))^2 + \epsilon}. \tag{2}$$

The style randomization (SR) module constructs randomized style features $\hat{\mu}, \hat{\sigma} \in \mathbb{R}^C$ by interpolating between the feature statistics of $\mathbf{z}$ and $\mathbf{z}'$. Then it replaces the style of the feature map $\mathbf{z}$ with the randomized style by applying adaptive instance normalization (AdaIN) [24]:

$$\hat{\mu} = \alpha\cdot\mu(\mathbf{z}) + (1-\alpha)\cdot\mu(\mathbf{z}'), \tag{3}$$

$$\hat{\sigma} = \alpha\cdot\sigma(\mathbf{z}) + (1-\alpha)\cdot\sigma(\mathbf{z}'), \tag{4}$$

$$\mathrm{SR}(\mathbf{z},\mathbf{z}') = \hat{\sigma}\cdot\left(\frac{\mathbf{z}-\mu(\mathbf{z})}{\sigma(\mathbf{z})}\right) + \hat{\mu}, \tag{5}$$

where $\alpha \sim \mathrm{Uniform}(0,1)$. The style-randomized feature map is fed into the content-biased network $\mathbf{G}_\mathrm{c}$. Finally, we obtain a content-biased loss L_c to predict one of the K categories with cross-entropy, which jointly optimizes the feature extractor $\mathbf{G}_\mathrm{f}$ and the content-biased network $\mathbf{G}_\mathrm{c}$:

$$\min_{\mathbf{G}_\mathrm{f},\mathbf{G}_\mathrm{c}} L_\mathrm{c} = -\mathbb{E}_{(\mathbf{x},\mathbf{y})\in S}\sum_{k=1}^{K}\mathbf{y}_k \log \mathbf{G}_\mathrm{c}(\mathrm{SR}(\mathbf{G}_\mathrm{f}(\mathbf{x}),\mathbf{z}'))_k, \tag{6}$$

where $\mathbf{y} \in \{0,1\}^K$ is the one-hot label for $\mathbf{x}$ and S is the training set.

By randomly blending the style features during training, the content-biased network can no longer rely on styles but focus on contents in making decisions. At test time, we disable SR and directly connect $\mathbf{G}_\mathrm{f}$ to $\mathbf{G}_\mathrm{c}$, which ensures independent

predictions and saves computation. Nevertheless, we found that applying SR at test time does not hurt the performance, which verifies that the model is trained to be invariant to the style features.

3.2 Adversarial Style-Biased Learning

In addition to the content-biased learning which ignores the style features, we further constrain the feature extractor from learning discriminative style features by adopting an adversarial learning framework. In other words, we make the style features encoded by the feature extractor to be incapable of discriminating the object class labels. To achieve this, we build an auxiliary style-biased network $\mathbf{G}_\text{s}$ as a discriminator to make a prediction based on styles, and let the feature extractor $\mathbf{G}_\text{f}$ to fool the style-biased network, which we call adversarial style-biased learning.

On contrary to SR which leaves the content of the input and randomizes its style, content randomization (CR) does the opposite: it maintains the style and switches the content to that of a randomly chosen image. Given intermediate feature maps $\mathbf{z}, \mathbf{z}' \in \mathbb{R}^{C\times H\times W}$ corresponding to the input $\mathbf{x}$ and the randomly chosen image $\mathbf{x}'$, we apply AdaIN to the content of $\mathbf{z}'$ with the style of $\mathbf{z}$:

$$\text{CR}(\mathbf{z}, \mathbf{z}') = \sigma(\mathbf{z}) \cdot \left(\frac{\mathbf{z}' - \mu(\mathbf{z}')}{\sigma(\mathbf{z}')} \right) + \mu(\mathbf{z}), \tag{7}$$

which can be interpreted as a content-randomized feature map of $\mathbf{z}$. It is taken as an input to the style-biased network $\mathbf{G}_\text{s}$ which is trained to make a style-biased prediction by minimizing a style-biased loss L_s:

$$\min_{\mathbf{G}_\text{s}} L_\text{s} = -\mathbb{E}_{(\mathbf{x},\mathbf{y})\in S} \sum_{k=1}^{K} \mathbf{y}_k \log \mathbf{G}_\text{s}(\text{CR}(\mathbf{G}_\text{f}(\mathbf{x}), \mathbf{z}'))_k. \tag{8}$$

The feature extractor $\mathbf{G}_\text{f}$ is then trained to fool $\mathbf{G}_\text{s}$ using an adversarial loss L_adv computed by the cross-entropy between the style-biased prediction and uniform distribution, which boils down to maximizing the entropy of the style-biased prediction[1]:

$$\min_{\mathbf{G}_\text{f}} L_\text{adv} = -\lambda_\text{adv} \cdot \mathbb{E}_{(\mathbf{x},\cdot)\in S} \sum_{k=1}^{K} \frac{1}{K} \log \mathbf{G}_\text{s}(\text{CR}(\mathbf{G}_\text{f}(\mathbf{x}), \mathbf{z}')))_k, \tag{9}$$

where λ_adv is a weighting coefficient.

The adversarial learning is performed with respect to only the affine transformation parameters (i.e. batch normalization parameters) in $\mathbf{G}_\text{f}$, which directly manipulate style features [24,27]. We can also effectively control the trade-off between the content and style biases by adjusting the coefficient λ_adv, which is explored in Sec. 4.1.

[1] We empirically found that matching with a uniform distribution provides more stable convergence than directly maximizing the entropy or using a gradient reversal layer [11].

Algorithm 1: Optimization Process of SagNets

Input: training data $S = (\mathbf{x}_i, \mathbf{y}_i)_{i=1}^{M}$; hyperparameter $\lambda_{\text{adv}} > 0$
Initialize: feature extractor $\mathbf{G}_\text{f}$; content-biased network $\mathbf{G}_\text{c}$; style-biased network $\mathbf{G}_\text{s}$
while *not converged* **do**
  $\mathbf{X}, \mathbf{Y} = \textsc{SampleBatch}(S, N)$ `// sample a minibatch of size` N
  $\mathbf{Z} = \mathbf{G}_\text{f}(\mathbf{X})$
  $\mathbf{Z}' = \textsc{Permutate}(\mathbf{Z})$ `// randomly permutate examples`
  Content-Biased Learning:
  $\mathbf{Z}^{(\text{c})} = \text{SR}(\mathbf{Z}, \mathbf{Z}')$ `// Eq. 5`
  $L_\text{c} = -\frac{1}{N}\sum_{j=1}^{N}\sum_{k=1}^{K}\mathbf{Y}_{jk}\log\mathbf{G}_\text{c}(\mathbf{Z}_j^{(\text{c})})_k$ `// Eq. 6`
  Minimize L_c w.r.t. $\mathbf{G}_\text{f}$ and $\mathbf{G}_\text{c}$
  Adversarial Style-Biased Learning:
  $\mathbf{Z}^{(\text{s})} = \text{CR}(\mathbf{Z}, \mathbf{Z}')$ `// Eq. 7`
  $L_\text{s} = -\frac{1}{N}\sum_{j=1}^{N}\sum_{k=1}^{K}\mathbf{Y}_{jk}\log\mathbf{G}_\text{s}(\mathbf{Z}_j^{(\text{s})})_k$ `// Eq. 8`
  Minimize L_c w.r.t. $\mathbf{G}_\text{s}$
  $L_\text{adv} = -\lambda_\text{adv}\cdot\frac{1}{N}\sum_{j=1}^{N}\sum_{k=1}^{K}\frac{1}{K}\log\mathbf{G}_\text{s}(\mathbf{Z}_j^{(\text{s})})_k$ `// Eq. 9`
  Minimize L_adv w.r.t. $\mathbf{G}_\text{f}$
end
Output: $\mathbf{G}_\text{c} \circ \mathbf{G}_\text{f}$

3.3 Implementation Details

Our framework can be readily integrated into modern CNN architectures and trained end-to-end. Given a CNN such as a ResNet [19], the feature extractor $\mathbf{G}_\text{f}$ comprises first few stages[2] of the CNN, while the rest of the network becomes the content-biased network $\mathbf{G}_\text{c}$; the style-biased network $\mathbf{G}_\text{s}$ forms the same structure as $\mathbf{G}_\text{c}$. Consequently, the output network $\mathbf{G}_\text{c} \circ \mathbf{G}_\text{f}$ has exactly the same architecture as the original CNN—in other words, it does not impose any overhead in terms of both parameters and computations at test time. To minimize the computational overhead during training, we choose the random image within a minibatch: given intermediate feature maps $\mathbf{Z} \in \mathbb{R}^{N\times C\times H\times W}$ from a minibatch of size N, we construct feature maps of arbitrary images $\mathbf{Z}'$ by simply permutating $\mathbf{Z}$ along the batch dimension. The overall training procedure of SagNets is summarized in Algorithm 1.

3.4 Extension to Un/Semi-Supervised Learning

Although our framework does not require training data from the target domain, some problem settings such as un/semi-supervised domain adaptation allow access to unlabeled target data for training. To fully leverage those unlabeled data,

[2] A stage refers to a group of layers that share the same feature map size.

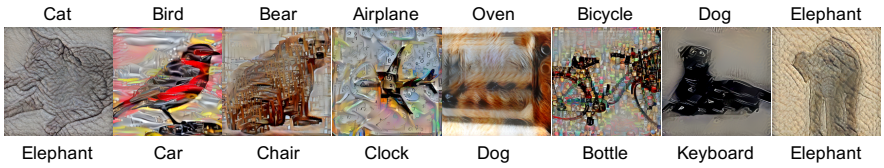

Fig. 3: Examples of the texture-shape cue conflict stimuli [14] with their shape (top) and texture (bottom) labels.

we propose a simple extension of SagNets based on consistency learning [38,49]. For each training example $\mathbf{x}$ from a set of unlabeled data S_{unl}, we obtain two prediction vectors from the network: one applied SR and the other not applied SR. The inconsistency between the two final predictions are estimated by the mean square error and minimized for all unlabeled data:

$$\min_{\mathbf{G}_\text{f},\mathbf{G}_\text{c}} L_{\text{unl}} = \lambda_{\text{unl}} \cdot \mathbb{E}_{\mathbf{x}\in S_{\text{unl}}} \sum_{k=1}^{K} \left(\mathbf{G}_\text{c}(\text{SR}(\mathbf{G}_\text{f}(\mathbf{x}), \mathbf{z}'))_k - \mathbf{G}_\text{c}(\mathbf{G}_\text{f}(\mathbf{x}))_k\right)^2, \quad (10)$$

where λ_{unl} is the corresponding coefficient which is set to 0.01. Furthermore, our adversarial learning is naturally extended to unlabeled data because the adversarial loss (Eq. 9) does not require ground-truth labels.

4 Experiments

In this section, we first conduct an experimental analysis to gain an insight into the effect of SagNets (Sec. 4.1), then perform comprehensive evaluation on a wide range of cross-domain tasks including domain generalization (DG) (Sec. 4.2), unsupervised domain adaptation (UDA) (Sec. 4.3), and semi-supervised domain adaptation (SSDA) (Sec. 4.4) compared with state-of-the-art methods. All baseline networks are pretrained on ImageNet classification [44].

4.1 Biases and Domain Gap

We examine the effect of SagNets on the biases of CNNs and the discrepancy between domains using two datasets. **16-class-ImageNet** [15] is a subset of ImageNet containing 213,555 images from 16 entry-level categories. The **texture-shape cue conflict stimuli** [14] dataset is introduced to measure the biases of CNNs, which consists of 1,280 images and shares the same 16 categories as 16-class-ImageNet. The cue conflict stimuli are generated by blending the texture and shape from different images via style transfer [13] (see examples in Fig. 3), so that we can observe whether a CNN makes a decision based upon the texture or shape.

We train SagNets with a ResNet-18 baseline on the 16-class-ImageNet by SGD with batch size 256, momentum 0.9, weight decay 0.0001, initial learning

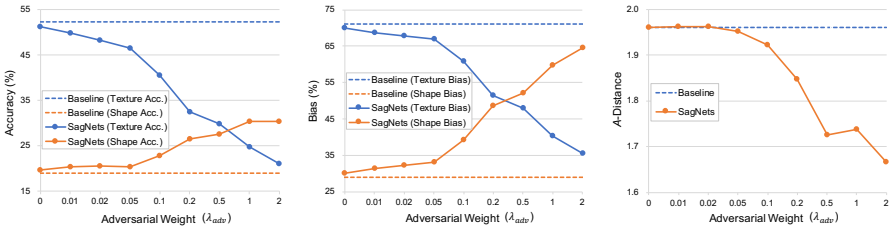

(a) Texture/shape acc. (b) Texture/shape bias (c) $\mathcal{A}$-distance

Fig. 4: The effect of SagNets on (a) texture/shape accuracy and (b) texture/shape bias on the cue conflict stimuli; (c) $\mathcal{A}$-distance between 16-class-ImageNet and the cue conflict stimuli. SagNets increase the shape accuracy as well as shape bias, and reduce the domain discrepancy.

rate 0.001, and cosine learning rate scheduling for 30 epochs. The randomization stage (the stage after which the randomizations are performed. i.e. the number of stages in the feature extractor) is set to 2, and we vary the adversarial coefficient λ_{adv}.

Texture/Shape Bias. As proposed in [13], we quantify the texture and shape biases of networks by evaluating them on the cue conflict stimuli and counting the number of predictions that correctly classify the texture or shape of images. For example, the shape bias is defined as the fraction of predictions matching the shape within the predictions matching either the shape or texture. The results clearly demonstrate that SagNets increase the shape accuracy and decrease the texture accuracy over the baseline (Fig. 4(a)), which consequently increase the shape bias and decrease the texture bias (Fig. 4(b)). Furthermore, the shape and texture biases are effectively controlled by the adversarial coefficient λ_{adv}, i.e. the shape bias increases as λ_{adv} increases. In practice, increasing λ_{adv} does not always improve the final classification accuracy (as in Fig. 5(b)), thus we need to find a fair trade-off.

Domain Gap. We further investigate the capability of SagNets in reducing domain discrepancy. We treat the 16-class-ImageNet and cue conflict stimuli dataset as two different domains because they share the same object categories but exhibit different appearances. Then, we measure the distance between the two domains using the features from the penultimate layer of the network. Following [34], we calculate a proxy $\mathcal{A}$-distance $d_{\mathcal{A}} = 2(1-\epsilon)$ where ϵ is a generalization error of an SVM classifier trained to distinguish the examples from the two domains. As illustrated in Fig. 4(c), SagNets effectively reduce the domain discrepancy as the adversarial weight increases. By plotting the $\mathcal{A}$-distance against the shape bias (Fig. 1), we observe an explicit correlation between the bias and domain gap: shape-biased representation generalizes better across domains, which confirms the common intuition [23,14,21].

Table 1: Multi-source DG accuracy (%) on the PACS dataset. Each column title indicates the target domain. The results of our DeepAll baseline and SagNets are averaged over three repetitions. SagNet$^{-\mathrm{CBL}}$ and SagNet$^{-\mathrm{ASBL}}$ refer to SagNets without content-biased learning and adversarial style-biased learning, respectively.

Backbone		Art paint.	Cartoon	Sketch	Photo	Avg.
AlexNet	D-SAM	63.87	70.70	64.66	85.55	71.20
	JiGen	67.63	71.71	65.18	89.00	73.38
	Epi-FCR	64.7	72.3	65.0	86.1	72.0
	MASF	70.35	72.46	67.33	**90.68**	75.21
	MMLD	69.27	**72.83**	66.44	88.98	74.38
	DeepAll	65.19	67.83	63.75	90.08	71.71
	SagNet	**71.01**	70.78	**70.26**	90.04	**75.52**
ResNet-18	D-SAM	77.33	72.43	**77.83**	95.30	80.72
	JiGen	79.42	75.25	71.35	96.03	80.51
	Epi-FCR	82.1	77.0	73.0	93.9	81.5
	MASF	80.29	77.17	71.69	94.99	81.04
	MMLD	81.28	77.16	72.29	**96.09**	81.83
	DeepAll	78.12	75.10	68.43	95.37	79.26
	SagNet$^{-\mathrm{CBL}}$	78.86	77.05	73.28	95.43	81.15
	SagNet$^{-\mathrm{ASBL}}$	82.94	76.73	74.74	95.07	82.37
	SagNet	**83.58**	**77.66**	76.30	95.47	**83.25**

Table 2: Multi-source DG accuracy (%) on the Office-Home dataset with a ResNet-18 backbone.

	Art	Clipart	Product	Real-World	Avg.
D-SAM	58.03	44.37	69.22	71.45	60.77
JiGen	53.04	**47.51**	**71.47**	72.79	61.20
DeepAll	58.51	41.44	70.06	73.28	60.82
SagNet	**60.20**	45.38	70.42	**73.38**	**62.34**

4.2 Domain Generalization

DG is a problem to train a model on a single or multiple source domain(s), and test on an unseen target domain. We evaluate the efficacy of SagNets against state-of-the-art DG methods including D-SAM [9], JiGen [5], Epi-FCR [31], MASF [8], and MMLD [37]. We adopt two datasets: **PACS** [30] consists of 9,991 images from 7 categories across 4 domains (Art Painting, Cartoon, Sketch, and Photo) and **Office-Home** [48] comprises 15,588 images from 65 categories and 4 domains (Art, Clipart, Product and Real-World). We split the training data of PACS into 70% training and 30% validation following the official split [30], and Office-Home into 90% training and 10% validation following [9]. Our networks are trained by SGD with batch size 96, momentum 0.9, weight decay 0.0001, initial learning rate 0.004 (0.002 with AlexNet) and cosine scheduling for 2K iterations (4K with AlexNet or Office-Home). The randomization stage and the

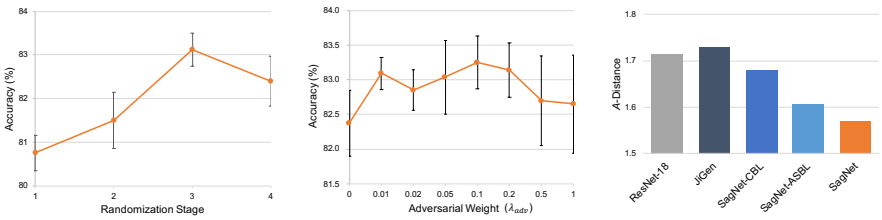

(a) Acc. *vs* random. stage (b) Acc. *vs* adv. weight (c) $\mathcal{A}$-distance

Fig. 5: Accuracy of SagNets on PACS with varying (a) randomization stage and (b) adversarial weight; (c) $\mathcal{A}$-distance between the source domains and target domain. Results are averaged over the 4 target domains and 3 repetitions, where error bars denote the standard deviation.

adversarial weight of SagNets are fixed to 3 and 0.1, respectively, throughout all remaining experiments unless otherwise specified.

Multi-Source Domain Generalization. We first examine multi-source DG where the model needs to generalize from multiple source domains to a novel target domain. We train our SagNets and the DeepAll baselines (i.e. naïve supervised learning) on the combination of all training data from the source domains regardless of their domain labels. Table 1 and 2 demonstrate that SagNets not only significantly improve the accuracy over the baselines but also outperform the competing methods. To the best of our knowledge, SagNets achieve new state-of-the-arts in both datasets. Furthermore, experiments without content-biased learning (SagNet^{-CBL}) and without adversarial style-biases learning (SagNet^{-ASBL}) verify the effectiveness of each component of SagNets. It is also worth noting that while all the compared methods except JiGen exploit additional layers on top of the baseline CNN at test time, SagNets do not require any extra parameters nor computations from the baseline.

Ablation. We perform elaborate ablation study for SagNets on multi-source DG using PACS. We first examine the effect of the randomization stage where the randomizations are applied, while keeping the adversarial weight to 0.1. Karras et al. [27] demonstrated that style features at different layers encode distinct visual attributes: style features from fine spatial resolutions (correspond to lower layers in our network) encode low-level attributes such as color and microtextures, while style features from coarse spatial resolutions (correspond to higher layers) encode high-level attributes such as global structures and macrotextures. In this regard, the randomization modules of SagNets need to be applied at a proper level, where the style features incur undesired bias. As shown in Fig. 5(a), SagNets offer the best accuracy when the randomizations are applied after stage 3, while randomizing too low-level styles is less helpful in reducing style bias; randomizing too high-level styles may lose important semantic information.

Table 3: Single-source DG accuracy (%) on the PACS dataset averaged over three repetitions (A: Art Painting, C: Cartoon, S: Sketch, P: Photo).

	A→C	A→S	A→P	C→A	C→S	C→P	S→A	S→C	S→P	P→A	P→C	P→S	Avg.
ResNet-18	59.1	49.2	**96.1**	65.1	65.6	84.3	27.2	37.2	39.7	66.3	26.8	34.7	54.3
JiGen	57.0	50.0	**96.1**	65.3	65.9	85.5	26.6	41.1	42.8	62.4	27.2	35.5	54.6
ResNet-18	62.3	49.0	95.2	65.7	60.7	83.6	28.0	54.5	35.6	64.1	23.6	29.1	54.3
SagNet	**67.1**	**56.8**	95.7	**72.1**	**69.2**	**85.7**	**41.1**	**62.9**	**46.2**	**69.8**	**35.1**	**40.7**	**61.9**

We also conduct ablation on the adversarial coefficient λ_{adv}, while the randomization stage is fixed to 3. Fig. 5(b) illustrates the accuracy of SagNets with varying magnitude of λ_{adv}. Although increasing λ_{adv} tends to steadily improve the shape bias as shown in Fig. 4(b), the actual performance peaks around $\lambda_{\text{adv}} = 0.1$. This indicates that while it is beneficial to increase the shape bias to some extent, it might harm the network in learning useful features to force excessive shape bias to the network.

Domain Gap. Reducing domain gap in DG settings is particularly challenging compared with other tasks such as UDA or SSDA since one can not make any use of the target distribution. To demonstrate the practicability of SagNets in reducing domain gap in such scenario, we measure the $\mathcal{A}$-distance between the source domains and the target domain following the same procedure as in Sec. 4.1; average over the 4 tasks of PACS. As shown in Fig. 5(c), SagNets considerably reduce the domain discrepancy compared to the ResNet-18 baseline and another state-of-the-art DG method JiGen[3].

Single-Source Domain Generalization. Our framework seamlessly extends to single-source DG where only a single training domain is provided, because it does not require domain labels nor multiple source domains (which are necessary in the majority of DG methods [30,9,31,8]). We train SagNets on each domain of PACS and evaluate them on the remaining domains. As reported in Table 3, SagNets remarkably boost the generalization performance, while JiGen[3] is theoretically applicable to single-source DG but fails to make a practical improvement.

4.3 Unsupervised Domain Adaptation

UDA is a task of transferring knowledge from a source to the target domain, where unlabeled target data are available for training. Besides the **Office-Home** dataset that we used for DG, we also employ **DomainNet** [43] which is a large-scale dataset containing about 0.6 million images from 6 domains and 345 categories.

[3] Reproduced with their official code (`https://github.com/fmcarlucci/JigenDG`) and the optimal hypterparameters provided in their paper.

Table 4: UDA accuracy (%) on the Office-Home dataset with a ResNet-50 backbone (A: Art, C: Clipart, P: Product, R: Real-World).

Method	SagNet	A→C	A→P	A→R	C→A	C→P	C→R	P→A	P→C	P→R	R→A	R→C	R→P	Avg.
ResNet-50		41.3	63.8	71.4	49.1	59.6	61.4	46.8	36.1	68.8	63.0	45.9	76.5	57.0
	✓	**45.7**	**64.1**	**72.6**	**49.6**	**60.0**	**63.5**	**49.9**	**40.7**	**71.1**	**64.8**	**50.9**	**78.1**	**59.2**
DANN		44.7	62.7	70.3	47.1	60.1	61.4	46.1	41.7	68.5	62.3	50.9	76.7	57.7
	✓	**48.8**	**65.2**	**71.4**	**50.3**	**61.4**	**62.5**	**50.7**	**45.7**	**71.8**	**65.4**	**55.2**	**78.6**	**60.6**
CDAN		50.6	69.0	**74.9**	54.6	66.1	67.9	57.2	46.9	75.6	69.1	55.8	**80.6**	64.0
	✓	**53.2**	**69.2**	**74.9**	**55.9**	**67.8**	**68.6**	**58.1**	**51.8**	**76.4**	**69.8**	**58.1**	80.4	**65.3**
CDAN+E		50.9	70.1	**76.5**	57.9	70.2	**70.6**	56.5	50.1	75.6	70.1	57.1	81.6	65.6
	✓	**55.8**	**71.5**	76.2	**59.7**	**70.9**	70.4	**59.2**	**54.6**	**77.1**	**71.0**	**60.3**	**82.4**	**67.4**

Table 5: UDA accuracy (%) on the DomainNet dataset with a ResNet-18 backbone (C: Clipart, P: Painting, S: Sketch, R: Real).

Method	SagNet	R→C	R→P	P→C	C→S	S→P	R→S	P→R	Avg.
ResNet-18		53.1	57.7	52.4	47.5	52.0	43.4	**68.5**	53.5
	✓	**54.4**	**58.0**	**53.1**	**49.2**	**52.2**	**46.4**	67.4	**54.4**
CDAN		53.0	57.4	52.3	48.0	52.3	43.4	**67.2**	53.4
	✓	**54.4**	**59.4**	**52.8**	**49.5**	**52.4**	**45.9**	67.1	**54.5**

Since some domains and classes are very noisy, we follow [45] to utilize its subset of 145,145 images from 4 domains (Clipart, Painting, Sketch, and Real) with 126 categories, and consider 7 adaptation scenarios. We demonstrate that SagNets not only boost the performance over the baseline, but also are seamlessly integrated into popular UDA methods such as DANN [11] and CDAN/CDAN+E [35] to make further improvements. We borrow the official implementation[4] of CDAN and its training policy, and reproduce all methods (i.e. ResNet, DANN, CDAN, CDAN+E, and their SagNet variants) on top of it for fair comparison.

As shown in Table 4, SagNets lead to impressive performance improvements when combined with any baseline method. Furthermore, while CDAN does not make meaningful improvement on DomainNet due to the complexity of the dataset in terms of scale and diversity, SagNets consistently improve the accuracy in most adaptation scenarios as presented in Table 5. These results suggest that the effectiveness of SagNets is orthogonal to existing approaches that explicitly align feature distributions, and generates a synergy by complementing them.

4.4 Semi-Supervised Domain Adaptation

We finally experiment on SSDA where a few target labels are provided, using the **DomainNet** dataset. Saito et al. [45] showed that common UDA methods [11,35,46] often fail to improve performance in such scenario and proposed MME, achieving the state-of-the-art for SSDA. Here we demonstrate that SagNets

[4] `https://github.com/thuml/CDAN`

Table 6: SSDA accuracy (%) on the DomainNet dataset (C: Clipart, P: Painting, S: Sketch, R: Real).

Backbone	Method	SagNet	R → C		R → P		P → C		C → S		S → P		R → S		P → R		Avg.	
			1-shot	3-shot	1-shot	3-shot	1-shot	3-shot	1-shot	3-shot	1-shot	3-shot	1-shot	3-shot	1-shot	3-shot	1-shot	3-shot
AlexNet	S+T		43.3	47.1	42.4	45.0	40.1	44.9	33.6	36.4	35.7	38.4	29.1	33.3	**55.8**	**58.7**	40.0	43.4
		✓	**45.8**	**49.1**	**45.6**	**46.7**	**42.7**	**46.3**	**36.1**	**39.4**	**37.1**	**39.8**	**34.2**	**37.5**	54.0	57.0	**42.2**	**45.1**
	MME		48.9	55.6	48.0	49.0	46.7	51.7	36.3	39.4	39.4	43.0	33.3	37.9	56.8	**60.7**	44.2	48.2
		✓	**54.1**	**58.6**	**49.8**	**52.2**	**48.7**	**54.4**	**39.6**	**43.4**	**40.4**	**43.4**	**39.7**	**42.8**	**57.0**	60.3	**47.0**	**50.7**
VGG-16	S+T		49.0	52.3	55.4	56.7	47.7	51.0	43.9	48.5	50.8	55.1	37.9	45.0	**69.0**	**71.7**	50.5	54.3
		✓	**51.8**	**54.9**	**57.8**	**59.4**	**50.4**	**54.2**	**48.9**	**52.9**	**53.1**	**56.3**	**45.6**	**49.4**	68.3	70.9	**53.7**	**56.9**
	MME		60.6	64.1	63.3	63.5	57.0	60.7	50.9	55.4	**60.5**	60.9	50.2	54.8	**72.2**	**75.3**	59.2	62.1
		✓	**64.9**	**67.8**	**64.5**	**66.0**	**60.4**	**65.8**	**54.7**	**59.0**	59.8	**62.0**	**56.6**	**59.6**	71.1	74.2	**61.7**	**64.9**
ResNet-34	S+T		55.6	60.0	60.6	62.2	56.8	59.4	50.8	55.0	56.0	**59.5**	46.3	50.1	71.8	**73.9**	56.9	60.0
		✓	**59.4**	**62.0**	**61.9**	**62.9**	**59.1**	**61.5**	**54.0**	**57.1**	**56.6**	59.0	**49.7**	**54.4**	**72.2**	73.4	**59.0**	**61.5**
	MME		70.0	72.2	67.7	69.7	69.0	71.7	56.3	61.8	64.8	66.8	61.0	61.9	**76.1**	**78.5**	66.4	68.9
		✓	**72.3**	**74.2**	**69.0**	**70.5**	**70.8**	**73.2**	**61.7**	**64.6**	**66.9**	**68.3**	**64.3**	**66.1**	75.3	78.4	**68.6**	**70.8**

not only bring considerable improvements over the baseline, but also further improve the performance of MME. For a fair comparison, SagNets are built upon the official implementation of MME[5], trained with the same training policy and the few-shot labels specified by [45].

Table 6 illustrates the results of SSDA with various architectures, where S+T [6] indicates a baseline few-shot learning algorithm based on cosine similarity learning. Our method consistently enhances the performance with considerable margins across all tested architectures, which verifies its scalability with respect to model variety. Furthermore, SagNets achieve compelling improvements in most settings for both S+T and MME, setting a new state-of-the-art for SSDA when combined with MME.

5 Conclusion

We present Style-Agnostic Networks (SagNets) that are robust against domain shifts caused by style variation across domains. By randomizing styles in a latent feature space and adversarially deactivating styles of the feature extractor, SagNets are trained to concentrate more on contents rather than styles in their decision-making process. Our extensive experiments confirm the effectiveness of SagNets in controlling the biases of CNNs and reducing the discrepancy across domains in a broad range of problem settings. The proposed framework is also orthogonal to many existing domain adaptation methods that explicitly align distributions of different domains, which is verified by complementarily achieving further improvements along with those approaches. The principle of how we deal with the intrinsic biases of CNNs can be applied to other areas such as improving robustness under image corruptions [20] or defending against adversarial attacks [18], which are left for future investigation.

[5] `https://github.com/VisionLearningGroup/SSDA_MME`

References

1. Baker, N., Lu, H., Erlikhman, G., Kellman, P.J.: Deep convolutional networks do not classify based on global object shape. PLOS Computational Biology (2018)
2. Balaji, Y., Sankaranarayanan, S., Chellappa, R.: Metareg: Towards domain generalization using meta-regularization. In: NeurIPS (2018)
3. Ballester, P., Araujo, R.M.: On the performance of googlenet and alexnet applied to sketches. In: AAAI (2016)
4. Ben-David, S., Blitzer, J., Crammer, K., Pereira, F.: Analysis of representations for domain adaptation. In: NIPS (2007)
5. Carlucci, F.M., D'Innocente, A., Bucci, S., Caputo, B., Tommasi, T.: Domain generalization by solving jigsaw puzzles. In: CVPR (2019)
6. Chen, W.Y., Liu, Y.C., Kira, Z., Wang, Y.C., Huang, J.B.: A closer look at few-shot classification. In: ICLR (2019)
7. Donahue, J., Hoffman, J., Rodner, E., Saenko, K., Darrell, T.: Semi-supervised domain adaptation with instance constraints. In: CVPR (2013)
8. Dou, Q., de Castro, D.C., Kamnitsas, K., Glocker, B.: Domain generalization via model-agnostic learning of semantic features. In: NeurIPS (2019)
9. DInnocente, A., Caputo, B.: Domain generalization with domain-specific aggregation modules. In: GCPR (2018)
10. Ganea, P.A., Pickard, M.B., DeLoache, J.S.: Transfer between picture books and the real world by very young children. Journal of Cognition and Development (2008)
11. Ganin, Y., Ustinova, E., Ajakan, H., Germain, P., Larochelle, H., Laviolette, F., Marchand, M., Lempitsky, V.: Domain-adversarial training of neural networks. JMLR (2016)
12. Gatys, L., Ecker, A.S., Bethge, M.: Texture synthesis using convolutional neural networks. In: NIPS (2015)
13. Gatys, L.A., Ecker, A.S., Bethge, M.: Image style transfer using convolutional neural networks. In: CVPR (2016)
14. Geirhos, R., Rubisch, P., Michaelis, C., Bethge, M., Wichmann, F.A., Brendel, W.: Imagenet-trained cnns are biased towards texture; increasing shape bias improves accuracy and robustness. In: ICLR (2019)
15. Geirhos, R., Temme, C.R., Rauber, J., Schütt, H.H., Bethge, M., Wichmann, F.A.: Generalisation in humans and deep neural networks. In: NeurIPS (2018)
16. Ghifary, M., Balduzzi, D., Kleijn, W.B., Zhang, M.: Scatter component analysis: A unified framework for domain adaptation and domain generalization. TPAMI (2016)
17. Ghifary, M., Kleijn, W.B., Zhang, M.: Domain adaptive neural networks for object recognition. In: PRICAI (2014)
18. Goodfellow, I.J., Shlens, J., Szegedy, C.: Explaining and harnessing adversarial examples. In: ICLR (2015)
19. He, K., Zhang, X., Ren, S., Sun, J.: Deep residual learning for image recognition. In: CVPR (2016)
20. Hendrycks, D., Dietterich, T.: Benchmarking neural network robustness to common corruptions and perturbations. In: ICLR (2019)
21. Hermann, K.L., Kornblith, S.: Exploring the origins and prevalence of texture bias in convolutional neural networks. arXiv preprint arXiv:1911.09071 (2019)
22. Hoffman, J., Tzeng, E., Park, T., Zhu, J.Y., Isola, P., Saenko, K., Efros, A.A., Darrell, T.: Cycada: Cycle consistent adversarial domain adaptation. In: ICML (2018)

23. Hosseini, H., Xiao, B., Jaiswal, M., Poovendran, R.: Assessing shape bias property of convolutional neural networks. In: CVPR Workshops (2018)
24. Huang, X., Belongie, S.: Arbitrary style transfer in real-time with adaptive instance normalization. In: ICCV (2017)
25. cnns with bag-of-local-features models works surprisingly well on imagenet, A.: Brendel, wieland and bethge, matthias. In: ICLR (2019)
26. Johnson, J., Alahi, A., Fei-Fei, L.: Perceptual losses for real-time style transfer and super-resolution. In: ECCV (2016)
27. Karras, T., Laine, S., Aila, T.: A style-based generator architecture for generative adversarial networks. In: CVPR (2019)
28. Landau, B., Smith, L.B., Jones, S.S.: The importance of shape in early lexical learning. Journal of Cognition and Development (1988)
29. Lee, H., Kim, H.E., Nam, H.: Srm: A style-based recalibration module for convolutional neural networks. In: ICCV (2019)
30. Li, D., Yang, Y., Song, Y.Z., Hospedales, T.M.: Deeper, broader and artier domain generalization. In: ICCV (2017)
31. Li, D., Zhang, J., Yang, Y., Liu, C., Song, Y.Z., Hospedales, T.M.: Episodic training for domain generalization. In: ICCV (October 2019)
32. Li, H., Jialin Pan, S., Wang, S., Kot, A.C.: Domain generalization with adversarial feature learning. In: CVPR (2018)
33. Li, Y., Tian, X., Gong, M., Liu, Y., Liu, T., Zhang, K., Tao, D.: Deep domain generalization via conditional invariant adversarial networks. In: ECCV (2018)
34. Long, M., Cao, Y., Wang, J., Jordan, M.I.: Learning transferable features with deep adaptation networks. In: ICML (2015)
35. Long, M., Cao, Z., Wang, J., Jordan, M.I.: Conditional adversarial domain adaptation. In: NeurIPS (2018)
36. Long, M., Zhu, H., Wang, J., Jordan, M.I.: Deep transfer learning with joint adaptation networks. In: ICML (2017)
37. Matsuura, T., Harada, T.: Domain generalization using a mixture of multiple latent domains. In: AAAI (2020)
38. Miyato, T., Maeda, S.i., Koyama, M., Ishii, S.: Virtual adversarial training: a regularization method for supervised and semi-supervised learning. TPAMI (2018)
39. Muandet, K., Balduzzi, D., Schölkopf, B.: Domain generalization via invariant feature representation. In: ICML (2013)
40. Murez, Z., Kolouri, S., Kriegman, D., Ramamoorthi, R., Kim, K.: Image to image translation for domain adaptation. In: CVPR (2018)
41. Nam, H., Kim, H.E.: Batch-instance normalization for adaptively style-invariant neural networks. In: NeurIPS (2018)
42. Pan, S.J., Yang, Q.: A survey on transfer learning. TKDE (2009)
43. Peng, X., Bai, Q., Xia, X., Huang, Z., Saenko, K., Wang, B.: Moment matching for multi-source domain adaptation. In: ICCV (2019)
44. Russakovsky, O., Deng, J., Su, H., Krause, J., Satheesh, S., Ma, S., Huang, Z., Karpathy, A., Khosla, A., Bernstein, M., et al.: Imagenet large scale visual recognition challenge. IJCV (2015)
45. Saito, K., Kim, D., Sclaroff, S., Darrell, T., Saenko, K.: Semi-supervised domain adaptation via minimax entropy. In: ICCV (2019)
46. Saito, K., Ushiku, Y., Harada, T., Saenko, K.: Adversarial dropout regularization. In: ICLR (2018)
47. Tzeng, E., Hoffman, J., Saenko, K., Darrell, T.: Adversarial discriminative domain adaptation. In: CVPR (2017)

48. Venkateswara, H., Eusebio, J., Chakraborty, S., Panchanathan, S.: Deep hashing network for unsupervised domain adaptation. In: CVPR (2017)
49. Xie, S., Zheng, Z., Chen, L., Chen, C.: Learning semantic representations for unsupervised domain adaptation. In: ICML (2018)
50. Yao, T., Pan, Y., Ngo, C.W., Li, H., Mei, T.: Semi-supervised domain adaptation with subspace learning for visual recognition. In: CVPR (2015)